Nanostructures

DOI: 10.1002/anie.201203456

Diffusion through the Shells of Yolk–Shell and Core–Shell Nanostructures in the Liquid Phase**

*Xiaoliang Liang, Jie Li, Ji Bong Joo, Alejandro Gutiérrez, Aashani Tillekaratne, Ilkeun Lee, Yadong Yin, and Francisco Zaera**

Recent advances in synthetic materials sciences such as the incorporation of self-assembly, sol–gel, and layer-by-layer deposition chemistry have afforded the development of many interesting and potentially useful nanostructures. Among those, nanoarchitectures in which a core nanoparticle, often a transition metal, is encapsulated by an outer layer of a second material, typically a porous oxide, have gained much popularity recently. The shells in these so-called core–shell nanostructures can offer a number of functionalities, including protection of the core from the outside environment, help in maintaining its compositional and structural integrity, prevention of the core from aggregating or sintering into larger particles, selective percolation of molecules in and out of the interior of the shell, increases in solubility and/or biocompatibility, and addition of new physical or chemical properties.[1–3] More sophisticated nanostructures can also be synthesized with a void space, in a yolk–shell or rattle-type nanoarchitecture, to create individualized nanoreactors around the core nanoparticles.[4–6] The new properties of these nanostructures have already been exploited in sensing,[7,8] drug delivery and biomedical imaging,[9–11] catalysis and electrocatalysis (including fuel cells),[12–14] and the development of batteries[15] and energy storage devices.[16]

Although many of the applications of the core–shell and yolk–shell nanostructures require the diffusion of molecules through the outer shell to the core nanoparticle, often the active phase, surprisingly little work has been reported on the direct characterization of mass transport across such shells. Only a couple of examples have been reported in the gas phase, where IR absorption spectroscopy has been used to confirm adsorption of carbon monoxide on the core element of Pt@CoO[17] and Au@TiO_2[18] yolk–shell samples. Herein we present what we believe is the first study on the accessibility of the core nanoparticles in these types of systems in liquid phase, an environment that is experimentally more difficult to probe.[19] We have used both carbon monoxide and cinchonidine in the liquid solvent (carbon tetrachloride) as probes to assess the possible availability of the inner surfaces of Pt@void@TiO_2 yolk–shell and Pt@SiO_2 core–shell nanostructures.

We first turn our attention to the Pt@void@TiO_2 yolk–shell nanostructure, a transmission electron microscopy (TEM) image of which is provided in Figure 1c. Its performance was evaluated in contrast with appropriate reference materials, namely, void@TiO_2 hollow shells (Figure 1a), a void@TiO_2@SiO_2 hollow double-shell nanostructure (Figure 1b), and a regular 1 wt% Pt/TiO_2 catalyst prepared by

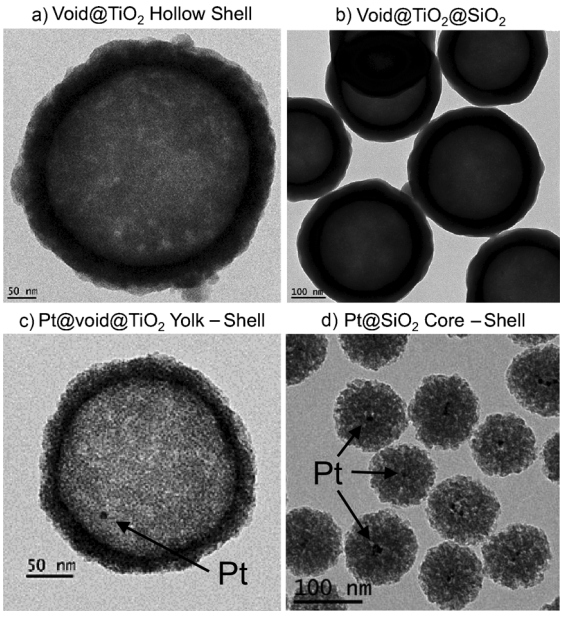

Figure 1. Transmission electron microscopy (TEM) images of the key samples studied herein: a) void@TiO_2 hollow shells (scale bar 50 nm); b) void@TiO_2@SiO_2 double-shell nanostructures (scale bar 100 nm); c) Pt@void@TiO_2 yolk–shell nanostructures; and d) Pt@SiO_2 core–shell nanostructures.

[*] X. Liang, J. Li, Dr. J. B. Joo, Dr. A. Gutiérrez, Dr. A. Tillekaratne, Dr. I. Lee, Prof. Y. Yin, Prof. F. Zaera
Department of Chemistry, University of California
Riverside, CA 92521 (USA)
E-mail: zaera@ucr.edu
Homepage: http://www.chem.ucr.edu/groups/Zaera/

X. Liang
Key Laboratory of Mineralogy and Metallogeny
Guangzhou Institute of Geochemistry
Chinese Academy of Sciences, Guangzhou 510640 (China)
and
Graduate University of the Chinese Academy of Sciences
Beijing 100049 (China)

Dr. A. Gutiérrez
Departamento de Física Aplicada
Universidad Autónoma de Madrid
Cantoblanco, 28049 Madrid (Spain)

[**] Financial assistance for this project was provided primarily by a grant from the US Department of Energy. Additional funding was provided by the US National Science Foundation. X.L. and J.L. acknowledge support from the China Scholarship Council, and A.G. acknowledges financial support from the Spanish Ministerio de Educación.

Supporting information for this article is available on the WWW under http://dx.doi.org/10.1002/anie.201203456.

dispersion of 5 nm Pt nanoparticles onto a commercial Degussa titania P-25 powder. The uptake of carbon monoxide on all those samples, all suspended in CCl_4, is indicated by the in situ IR absorption spectra in Figure 2a. Two general features are observed in those spectra at approximately 2070 and 2135 cm^{-1}, which correspond to the C–O stretching vibration of CO adsorbed on platinum and titania sites, respectively.

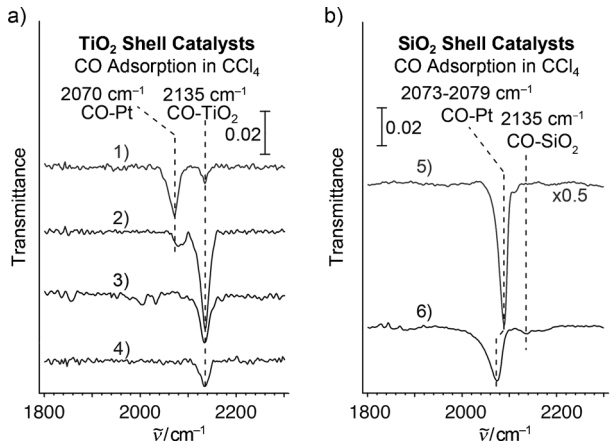

Figure 2. In situ transmission IR absorption spectra in the C–O stretching region for solid samples suspended in CCl_4 after room-temperature exposure to carbon monoxide. a) TiO_2 shell catalysts: 1) 1 mg of a supported 1 wt% Pt/TiO_2-P25 catalyst; 2) 8 mg of our Pt@void@TiO_2 yolk–shell nanostructure; 3) 3 mg of void@TiO_2 hollow shells; and 4) 3 mg of the void@TiO_2@SiO_2 hollow double-shell structure. b) SiO_2 shell catalysts: 5) 1 mg of a supported 1 wt% Pt/SiO_2 catalyst (top trace), and 6) 3 mg of our Pt@SiO_2 core–shell nanostructure (bottom).

A couple of observations from these data are worth mentioning. The first is that CO adsorption is indeed possible on the platinum nanoparticles embedded inside the titania shells in the Pt@void@TiO_2 sample. In fact, full access is indicated by the extent of that adsorption: the metal loading measured in the Pt@void@TiO_2 by comparison between the intensities of the CO IR peak at 2070 cm^{-1} obtained with that sample versus with Pt/TiO_2-P25, approximately (0.04 ± 0.01) wt%, compares well with the value estimated by calculations based on the geometry and density of the Pt nanoparticles and titania shells (ca. 0.03 wt%). Clearly, these data indicate that the inside of the titania shells are readily accessible to the carbon monoxide dissolved in the CCl_4 liquid.

The second observation worth discussing from the data in Figure 2a is that, in all the samples based on titania shells, CO adsorption on the titania itself occurs mainly on their external surfaces, not in the pores within the solid. This is despite the fact that those materials are quite porous and have large surface areas.[20] One key observation in connection with this conclusion is the remaining intensity (approximately half) seen in the CO peak at 2135 cm^{-1} with the void@TiO_2@SiO_2 sample. Adsorption there must occur at the inner surface of the shell, because all other surfaces have been blocked by the silica added by the sol–gel process used in its preparation. Indeed, the measured BET area drops from approximately 430 $m^2 g^{-1}$ in the void@TiO_2 sample to about 3 $m^2 g^{-1}$ in the case of the void@TiO_2@SiO_2 (Supporting Information, Figures S1, S2), a value even lower than that estimated for the inner surface of the shells by using geometrical arguments and the density of bulk titania (approximately 10–20 $m^2 g^{-1}$). It may very well be that the volume available inside the micropores of the titania shells is too small for CO adsorption (1–2 nm in diameter on average, according to the BET measurements; Supporting Information, Figure S1).

The fact that extensive CO adsorption is seen with the void@TiO_2@SiO_2 sample, where the micropores are all blocked, also suggests that the mechanism of diffusion through the oxide shells is dominated by transport at the grain boundaries. This conclusion was further confirmed by experiments using samples with crystalline shells,[21,22] where the microporous structure inherent to the sol–gel process was made to collapse at the expense of the formation of crystalline nanograins. The surface area of those crystalline samples is slightly lower (ca. 350 $m^2 g^{-1}$) and the pores larger (3–4 nm in diameter) that in the amorphous shells (Supporting Information, Figure S3); however, their performance in these CO adsorption experiments was similar, indicating comparable accessibility to the metal nanoparticles inside the shells in spite of the absence of microporosity.

CO adsorption was also tested on the Pt@SiO_2 core–shell structure shown in Figure 1d, which has no void space in between the Pt and SiO_2 layers. The porosity of this silica shell was indicated by the extensive CO adsorption that takes place on the Pt nanoparticles, as evidenced by the intense IR peak seen at 2073 cm^{-1} (Figure 2b, bottom trace). A 1 wt% Pt/SiO_2 (Aerosil 200) standard catalyst was also probed for reference. One other clear observation deriving from comparison of the IR data from all the samples studied here is that much more CO adsorption takes place on Pt/SiO_2 than on Pt/TiO_2 (Figure 2). This is an expected behavior reported previously and ascribed to the strong metal–support interaction (SMSI) effect seen with titania and other reducible oxides.[23,24] A slight shift in C–O stretching frequency is also seen in Figure 2b between the Pt/SiO_2 and Pt@SiO_2 samples. That may be explained by differences in coverage, but may also indicate an effect exerted by silica when in intimate contact with the platinum surface.

The diffusion through titania and silica shells reported here appears to be general, as it has been seen with other gases and with dissolved solids as well. For instance, it was observed that room-temperature oxidation of the CO adsorbed on the platinum nanoparticles can be achieved by subsequent exposure of the samples to O_2, bubbled into a fresh CCl_4 solution; this was indicated by both the disappearance of the C–O stretching peak and the detection of new features at around 2300–2400 cm^{-1} from dissolved CO_2. Furthermore, adsorption of CO on the Pt core of our samples is also possible in other solvents, such as ethanol. Finally, larger molecules, such as cinchonidine, an alkaloid often used in chiral catalysis,[25,26] can be adsorbed on the surface of the Pt nanoparticles inside the Pt@void@TiO_2 and Pt@SiO_2 nanostructures as well. This is illustrated by the data in Figure 3, where IR absorption peaks at approximately

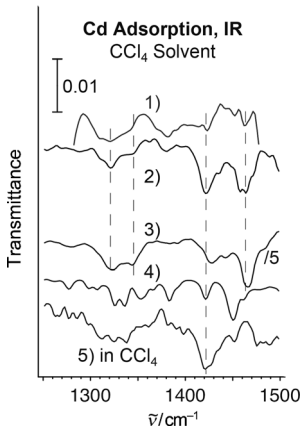

Figure 3. In situ transmission IR absorption spectra for cinchonidine adsorbed from a CCl_4 solution onto the solid samples. Top two traces: 1) Pt–void@TiO_2 and 2) Pt@SiO_2 nanostructures discussed herein; bottom three reference traces: 3) cinchonidine adsorbed from solution onto a Pt foil, 4) cinchonidine in pure form (as a solid), and 5) cinchonidine in a CCl_4 solution.[29]

1320, 1345, 1423, and 1463 cm^{-1} are seen in the traces for both Pt@void@TiO_2 and Pt@SiO_2 samples. Those are associated with the benzene ring in-plane deformation, quinuclidine CH_2 wag, quinoline in-plane deformation, and quinuclidine CH_2 scissor vibrational modes of cinchonidine adsorbed on platinum surfaces, respectively, and provide clear proof that cinchonidine has reached the surface of the metal (reference data from adsorption on a Pt foil are provided for comparison).[27,28]

Overall, molecular diffusion in and out of these yolk–shell and core–shell nanostructures in the liquid phase appears to be facile. In fact, mass transport through the shells may be too fast for certain applications such as drug delivery, in which case additional steps would need to be taken to partially block the diffusion paths available in the original shell material. On the other hand, these high diffusion rates are good for many catalytic applications.

Experimental Section

Pt@void@TiO_2 was prepared by a method similar to that previously reported for forming Au@void@TiO_2 samples.[18] A sacrificial silica layer was first grown by a sol–gel process with tetraethyl orthosilicate (TEOS) on a citrate-stabilized 5 nm-diameter Pt colloidal nanoparticle formed with PVP as the surfactant. The outer titania shell was then grown on top using tetrabutyl titanate (TBOT), and the silica finally etched away using an aqueous solution of NaOH.[6,30] The structures used in this study were made with TiO_2 shells 200 nm in diameter and 20 nm in thickness (Figure 1c). Reference void@TiO_2 hollow shells (Figure 1a) and void@TiO_2@SiO_2 samples (Figure 1b) were prepared by skipping the first step, namely, forming the Pt nanoparticles. The Pt@SiO_2 core–shell samples (Figure 1d) were prepared by growing a SiO_2 layer around the Pt nanoparticles by a sol–gel process, adding a PVP surfactant to protect the outer layer, and etching with NaOH to create a porous structure.[6]

CO adsorption was followed by using a previously developed in situ IR absorption spectroscopy cell,[31] modified to operate in transmission mode by using a polished surface of copper as a mirror in the back of the cell, and by trapping a suspension of the catalysts in solution in between that mirror and the front optical prism.[31,32]

More details are provided in the Supporting Information.

Received: May 4, 2012
Published online: June 29, 2012

Keywords: adsorption · diffusion · IR spectroscopy · mass transport · yolk–shell structures

[1] F. Caruso, *Adv. Mater.* **2001**, *13*, 11.
[2] P. Reiss, M. Protière, L. Li, *Small* **2009**, *5*, 154.
[3] W. Schärtl, *Nanoscale* **2010**, *2*, 829.
[4] Y. Yin, R. M. Rioux, C. K. Erdonmez, S. Hughes, G. A. Somorjai, A. P. Alivisatos, *Science* **2004**, *304*, 711.
[5] X. W. Lou, L. A. Archer, Z. Yang, *Adv. Mater.* **2008**, *20*, 3987.
[6] Q. Zhang, I. Lee, J. Ge, F. Zaera, Y. Yin, *Adv. Funct. Mater.* **2010**, *20*, 2201.
[7] A. Burns, H. Ow, U. Wiesner, *Chem. Soc. Rev.* **2006**, *35*, 1028.
[8] J.-H. Lee, *Sens. Actuators B* **2009**, *140*, 319.
[9] L. R. Hirsch, J. B. Jackson, A. Lee, N. J. Halas, J. L. West, *Anal. Chem.* **2003**, *75*, 2377.
[10] Y. Zhu, J. Shi, W. Shen, X. Dong, J. Feng, M. Ruan, Y. Li, *Angew. Chem.* **2005**, *117*, 5213; *Angew. Chem. Int. Ed.* **2005**, *44*, 5083.
[11] J. Gao, G. Liang, B. Zhang, Y. Kuang, X. Zhang, B. Xu, *J. Am. Chem. Soc.* **2007**, *129*, 1428.
[12] J. Luo, L. Wang, D. Mott, P. N. Njoki, Y. Lin, T. He, Z. Xu, B. N. Wanjana, I. I. S. Lim, C.-J. Zhong, *Adv. Mater.* **2008**, *20*, 4342.
[13] L. De Rogatis, M. Cargnello, V. Gombac, B. Lorenzut, T. Montini, P. Fornasiero, *ChemSusChem* **2010**, *3*, 24.
[14] C.-J. Jia, F. Schüth, *Phys. Chem. Chem. Phys.* **2011**, *13*, 2457.
[15] L. Su, Y. Jing, Z. Zhou, *Nanoscale* **2011**, *3*, 3967.
[16] G. Oldfield, T. Ung, P. Mulvaney, *Adv. Mater.* **2000**, *12*, 1519.
[17] S. Kim, Y. Yin, A. P. Alivisatos, G. A. Somorjai, J. T. Yates, *J. Am. Chem. Soc.* **2007**, *129*, 9510.
[18] I. Lee, J. B. Joo, Y. Yin, F. Zaera, *Angew. Chem.* **2011**, *123*, 10390; *Angew. Chem. Int. Ed.* **2011**, *50*, 10208.
[19] F. Zaera, *Chem. Rev.* **2012**, *112*, 2920.
[20] R. D. Gonzalez, T. Lopez, R. Gomez, *Catal. Today* **1997**, *35*, 293.
[21] J. B. Joo, Q. Zhang, I. Lee, M. Dahl, F. Zaera, Y. Yin, *Adv. Funct. Mater.* **2012**, *22*, 166.
[22] J. B. Joo, Q. Zhang, M. Dahl, I. Lee, J. Goebl, F. Zaera, Y. Yin, *Energy Environ. Sci.* **2012**, *5*, 6321.
[23] M. A. Vannice, L. C. Hasselbring, B. Sen, *J. Catal.* **1986**, *97*, 66.
[24] P. Pillonel, S. Derrouiche, A. Bourane, F. Gaillard, P. Vernoux, D. Bianchi, *Appl. Catal. A* **2005**, *278*, 223.
[25] T. Mallat, E. Orglmeister, A. Baiker, *Chem. Rev.* **2007**, *107*, 4863.
[26] Z. Ma, F. Zaera in *Design of Heterogeneous Catalysis: New Approaches Based on Synthesis Characterization, and Modelling* (Ed.: U. S. Ozkan), Wiley-VCH, Weinheim, **2009**, pp. 113–140.
[27] W. Chu, R. J. LeBlanc, C. T. Williams, J. Kubota, F. Zaera, *J. Phys. Chem. B* **2003**, *107*, 14365.
[28] J. Lai, Z. Ma, L. Mink, L. J. Mueller, F. Zaera, *J. Phys. Chem. B* **2009**, *113*, 11696.
[29] Z. Ma, I. Lee, F. Zaera, *J. Am. Chem. Soc.* **2007**, *129*, 16083.
[30] I. Lee, M. A. Albiter, Q. Zhang, J. Ge, Y. Yin, F. Zaera, *Phys. Chem. Chem. Phys.* **2011**, *13*, 2449.
[31] J. Kubota, Z. Ma, F. Zaera, *Langmuir* **2003**, *19*, 3371.
[32] M. A. Albiter, R. M. Crooks, F. Zaera, *J. Phys. Chem. Lett.* **2010**, *1*, 38.
[33] D.-G. Norton, D. G. Vlachos, *Combust. Flame* **2004**, *138*, 97.

